IJPAS | INTERNATIONAL JOURNAL PURE AND APPLIED SCIENCES
ISSN: 2149-0910

Vol. 10(1); 37-46 (2024)
DOI: 10.29132/ijpas.1388624

Research Article

A Research on Electrode Applications: Synthesis of Nickel-Doped Graphene Oxide

Harun KAYA

Received: 09.11.2024

Accepted: 25.03.2024

Malatya Turgut Özal University, Faculty of Engineering and Natural Sciences, Department of Engineering Basic Sciences, Malatya, Türkiye; harun.kaya@ozal.edu.tr

Abstract: In today's technology, carbon-based materials (such as graphene, graphene oxide, carbon nanotubes, etc.) have become one of the most important research areas due to a large number of applications. Graphene oxide (GO) is being investigated in many applications, especially in the energy field. In this study, GO was synthesized by a modified Hummer's method. After the synthesis of GO, nickel addition to the structure was made by the hydrothermal method. The morphological and structural properties of the synthesized GO were characterized by scanning electron microscope (SEM), X-ray powder diffraction (XRD) and Brunauer–Emmett–Teller (BET). According to the BET results, the surface areas of untreated GO and Ni-doped graphene oxide after heat treatment at 360°C (Ni-doped GO 360) were calculated as 3.22 $m^2 g^{-1}$ and 228 $m^2 g^{-1}$, respectively. Electrochemical properties of GO and Ni-doped GO 360 were analyzed using cyclic voltammetry (CV), long term charge/discharge analysis and impedance spectroscopy. At the end of 1000 cycles, it was determined that the Ni-doped GO 360 electrode retained 76% of its initial capacitance.

Keywords: Electrochemical properties; electrode; graphene oxide; modified Hummers method

Elektrot Uygulamaları Üzerine Bir Araştırma: Nikel Katkılı Grafen Oksit Sentezi

Özet: Günümüz teknolojisinde karbon bazlı malzemeler (grafen, grafen oksit, karbon nanotüpler vb.) çok sayıda uygulama nedeniyle en önemli araştırma alanlarından biri haline gelmiştir. Grafen oksit (GO), özellikle enerji olmak üzere birçok alanda araştırılmaktadır. Bu çalışmada GO, modifiye Hummers yöntemi ile sentezlenmiştir. GO sentezinden sonra hidrotermal yöntemle yapıya nikel ilavesi yapılmıştır. Sentezlenen GO' nun morfolojik ve yapısal özellikleri taramalı elektron mikroskobu (SEM), X-ışını toz kırınımı (XRD) ve Brunauer–Emmett–Teller (BET) ile karakterize edilmiştir. BET sonuçlarına göre GO ve Ni katkılı 360°C'de ısıl işleme tabi tutulmuş GO'nun (Ni katkılı GO 360) yüzey alanları sırasıyla 3.22 $m^2 g^{-1}$ ve 228 $m^2 g^{-1}$ olarak hesaplanmıştır. GO ve Ni katkılı GO 360'ın elektrokimyasal özellikleri siklik voltametri (CV), uzun süreli şarj/deşarj analizi ve empedans spektroskopisi kullanılarak analiz edilmiştir. 1000 döngünün sonunda, Ni katkılı GO 360 elektrodunun başlangıç kapasitansının % 76'sını koruduğu belirlenmiştir.

Anahtar Kelimeler: Electrochemical properties; electrode; graphene oxide; modified Hummers method

1. Introduction

Graphite crystal, one of the common allotropes of carbon, exhibits a three-dimensional structure by connecting strong covalent bonds of carbon atoms decoupled in hexagonal shape and weak Van Der Walls bonds between the planes. Due to the weak Van Der Walls bonds, the layers can be separated from each other very quickly. Graphite has attracted much attention recently due to its low cost, easy availability, easy conversion of graphene oxide (GO) and its derivatives into composite materials and graphene [1].

GO is a carbon-based material with 2-dimensional, oxygen-containing functional groups, and it can easily transform into graphite oxide from the oxidation of graphite and then graphene oxide by the decomposition of numerous layers [2]. GO has a wide range of applications due to the presence of oxygen-containing functional groups in its structure, the ratio of carbon atoms that hybridize sp^2 to carbon atoms that hybridize sp^3 is controllable, it has adjustable electronic and optical properties, and it has hydrophilic properties [3, 4].

Graphene can be produced from graphite via chemical [5, 6], chemical vapor deposition (CVD) [7, 8], mechanical [9, 10] or electrochemical [11, 12] methods.

The most important disadvantages of GO production methods are toxic and dangerous chemicals and the appearance of many toxic gases in the resulting products. In the studies conducted so far, the Hummers method, which uses a strong oxidizing agent such as $KMnO_4$ instead of the very dangerous ClO_2 and sodium nitrate instead of nitric acid, which forms a smoky acid vapor and also shortens the reaction time, has been the most advantageous [13]. This method introduced graphite into the oxidation reaction with a mixture of $KMnO_4$, concentrated H_2SO_4 and $NaNO_3$. The Mn_2O_7 formed here is a natural oxidant species and selectively oxidizes unsaturated aliphatic double bonds on aromatic structures [14]. The disadvantage of this method is the formation of toxic gases such as NO_2 and N_2O_4. In addition, if the temperature rises above 95° C, there is a risk of explosion of $KMnO_4$ and it is challenging to remove Na^+ and NO^{3-} ions trapped in the crystal cage from the aqueous solution [15].

Therefore, in subsequent studies, the Hummers method has been modified and ways to reduce these disadvantages have been investigated [16]. In these studies, changes have been made, such as changing the reaction conditions, using K_2FeO_4 instead of $KMnO_4$, increasing the amount of concentrated acid instead of NaNO3, or using H_3PO_4 in combination with H_2SO_4 [17].

In this study, Ni was doped to the GO structure produced using the modified Hummers method. By applying heat treatment to the obtained structure, it was studied how its electrochemical properties changed. Hence, this study aims to provide a solution to the current energy challenges in today's world.

2. Material and Method

GO production from graphite particles was done by the Modified Hummers method. After dissolving 0.1 M $NiCl_2$ in 80 mlt 0.1 g graphene oxide solution which obtained by modified Hummers method and adding it to the teflon-lined reactor, the hydrothermal reaction was carried out in a vacuum oven at 150 °C for 2 hours. After 2 hours, the oven was turned off and allowed to cool to room temperature. The sample taken from the hydrothermal reactor was washed several times with pure water and ethanol and then dried at 70 °C for 24 hours. To the DTA/TGA analysis (Figure 1) of the Ni-doped sample, heat treatment was carried out at 360 °C to obtain the NiO phase. Heat-treated Ni-doped and undoped samples were turned into electrodes to examine their capacitive properties. Nickel Doped and undoped GO structure was used as the active material. It was ground until a homogeneous mixture of active material (90%) and PVDF (10%) was obtained. A certain amount of 1-Methyl-2-pyrrolidone (NMP) was added to this mixture and mixed until a slurry structure was formed. This mixture was dropped onto porous Ni with a total mass of 5 mg and dried in a vacuum oven at 90 °C and 20 mbar pressure for 24 hours.

The structure obtained after these operations used as a supercapacitor electrode and placed in a three-electrode cell where electrochemical measurements (cyclic voltammogram (CV), galvanostatic charge-discharge measurements (GCD), specific capacitance (Csp) measurements, etc.) performed.

3. Results and Discussion

DTA/TGA curves of GO and Ni-doped GO are shown in Figure 1. In Figure 1, weight losses are observed in two regions between 26-280°C and 280-530°C in the GO structure. A 13% mass loss in the first region depends on removing adsorbed water in the structure, and a 45% mass loss in the second region depends on removing unstable and stable functional oxygen groups in the environment [18, 19]. The DTA curves shown by the dashed line also confirm this situation.

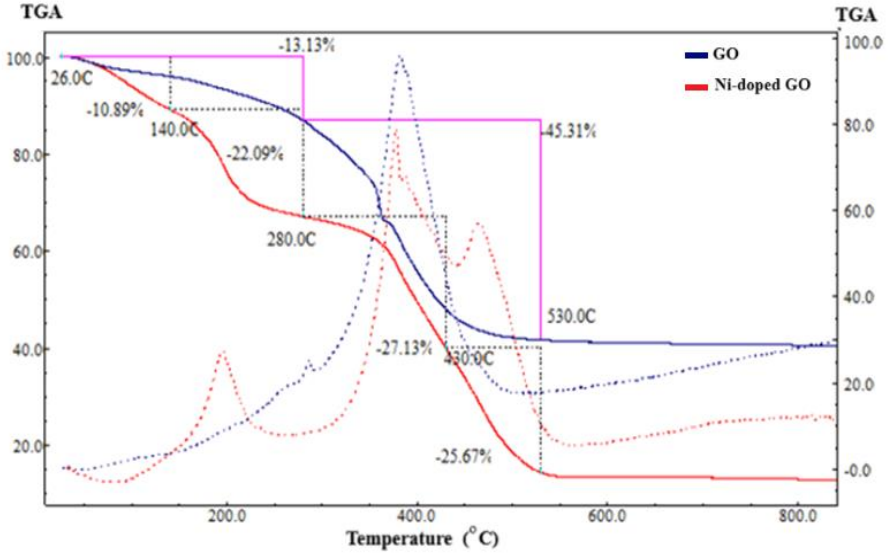

Figure 1. DTA/TGA curves of GO and Ni-doped GO.

The TGA curve shown in red indicates the Ni-doped GO. Mass loss is observed in four different regions. The mass loss occurring in 30-140°C, the first region, is due to the removal of moisture and ethanol in the environment. The second region, between 140-280°C, is caused by the thermal oxidative decaying of $Ni(OH)_2$ is considered. The third and fourth mass losses, located between 280-530°C, were caused by the environment's decaying of functional oxygen groups.

Figure 2 shows the curves of N_2 adsorption-desorption and change of pore width with pore digestion of the samples. All three examples show type IV isotherm according to the IUPAC classification. Micro and meso pores are located together in the structure.

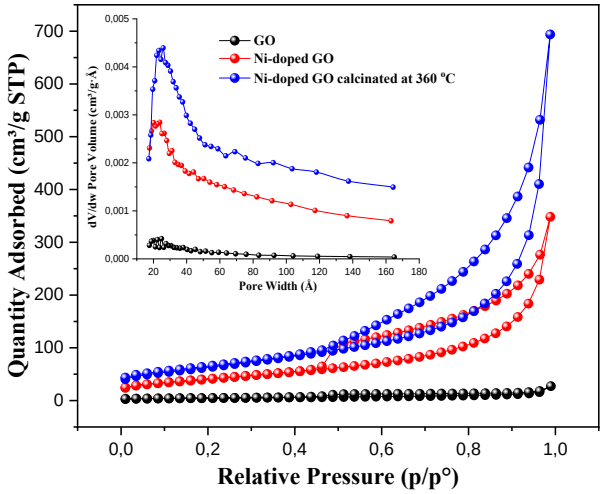

Figure 2. BET isotherm of GO, Ni-doped GO and Ni-doped GO 360.
(The graph on the inside shows the pore size distribution.)

Micro and meso pores are located together in the structure. Initially, the pores varying from 2-10 nm had a density, while the pore volume increased due to Ni addition to the structure, and 360°C heat treatment was observed. The surface areas determined according to BET measurements are 3 m^2 g^{-1}, 150 m^2 g^{-1} and 228 m^2 g^{-1} for GO, Ni-doped GO and Ni-doped GO 360, respectively.

Figure 3 shows the XRD spectra of the samples. The obtained spectrum for GO agrees with the literature [20-22]. As a result of the addition of Ni to the structure, peaks belonging to different nickel compounds have been observed. It has been determined that the NiO structure is formed due to applying heat treatment (calcinated) at 360°C.

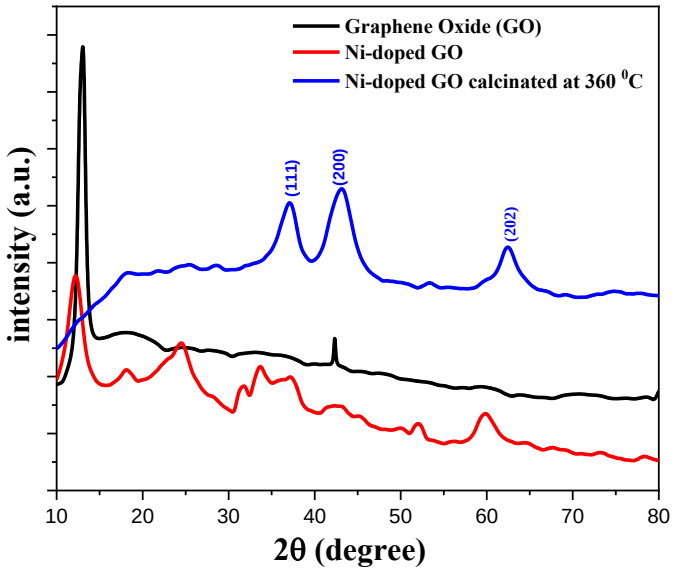

Figure 3. XRD spectra of GO, Ni-doped GO and Ni-doped GO 360.

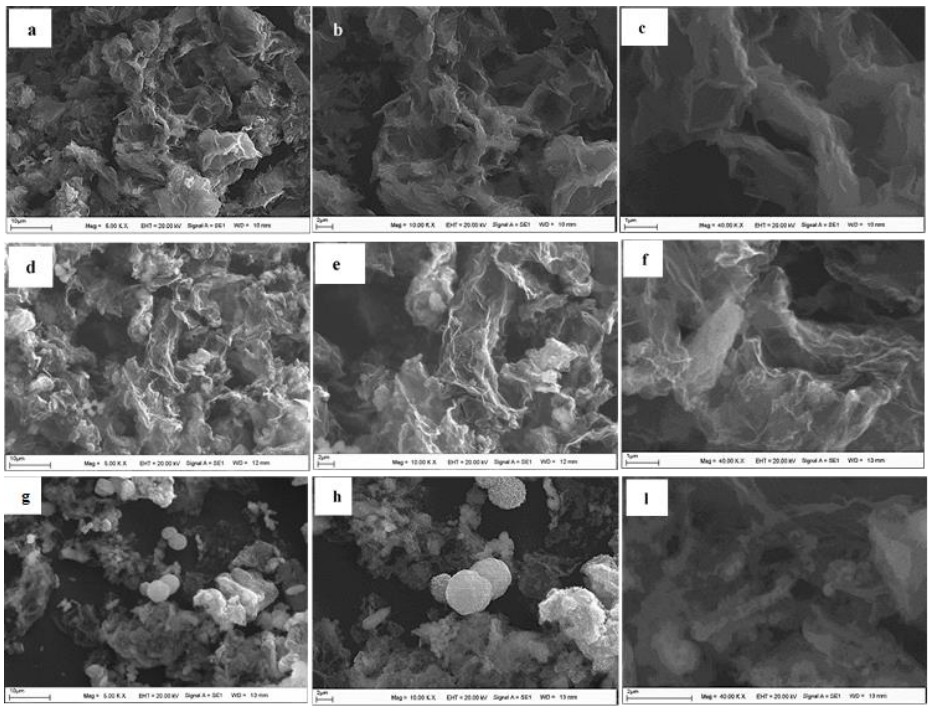

Figure 4. SEM images of a-c) GO d-f) Ni-doped GO g-i) Ni-doped GO 360.

GO structures obtained by the modified Hummers method are seen in Figure 4 a-c. The foliar and layered form of GO is visible. In Figure 4 d-f, the Ni-doped GO structure is present. Ni doping has occurred in GO in certain areas and widely. Figure 4 g-l shows the Ni-doped GO structure with heat treatment at 360°C. As a result of heat treatment, it has been observed that the Ni contained in the structure changes its form, and exhibits a leafy and spherical shape. This change in structure confirms the increase in surface area.

GO produced by the modified Hummers method (75%), Carbon Black (15%) and PVDF (10%) were thoroughly ground by mixing in a zirconium mortar for a certain period. Then, it was pressed after adding a certain amount to the Ni foam. The CV curves of the electrode prepared in this way at different scanning speeds in a 6 M KOH solution are given in Figure 5.

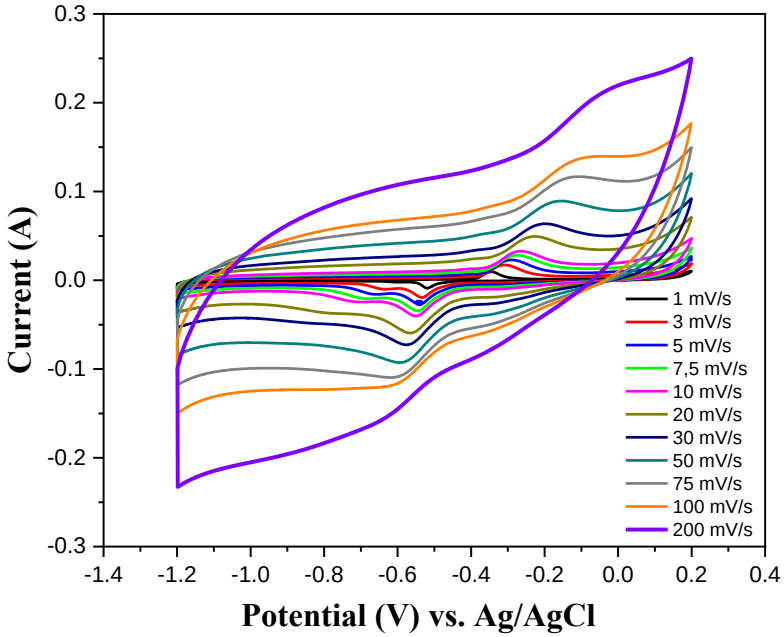

Figure 5. CV curves of the GO electrode at different scanning rates.

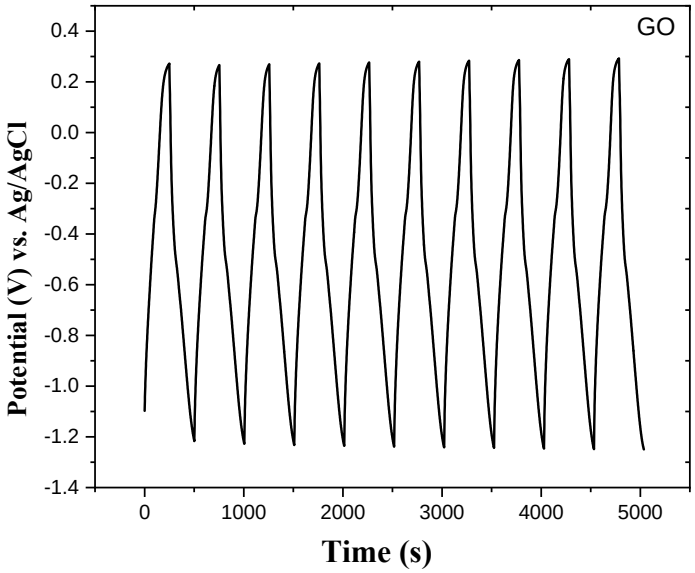

Figure 6. The first ten charge-discharge curves of the GO electrode.

Reduction and oxidation peaks around -0.6 and -0.2 are formed as a result of redox reactions between the electrode and the solution. These redox reactions indicate that the resulting electrode has pseudocapacitive behavior [23-25].

Figure 6 is the first ten charge-discharge curves taken in a three-electrode cell within 6 M KOH of the GO electrode. The fact that the curves obtained are in the shape of a sawtooth indicates that this electrode's capacitive behavior is good [26-29].

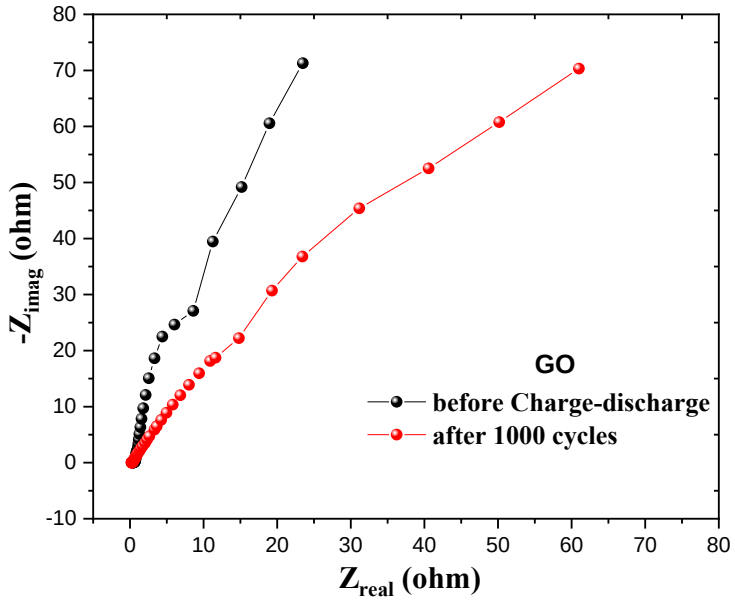

Figure 7. Electrochemical impedance spectroscopy curves at the open circuit potential of the GO electrode.

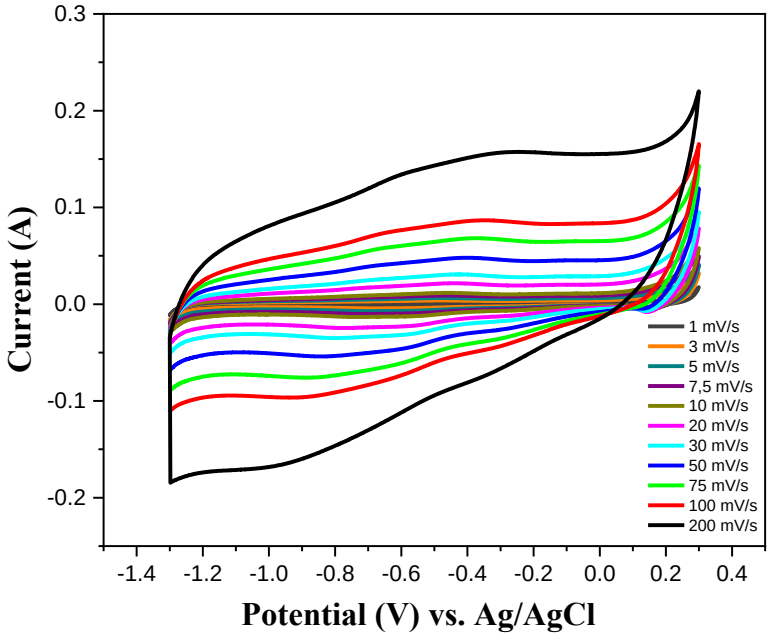

Figure 8. CV curves of the Ni-doped GO electrode at different scanning speeds.

Figure 7 shows the impedance spectra of the same electrode after the first and 1000 cycle charge-discharge process. The fact that the slopes of the curves obtained as a result of electrochemical impedance spectroscopy are more than 45° is associated with the suitable capacitive property of the electrode [30-32]. The slope of the electrochemical impedance curves of the GO electrode used in the study was initially around 70°. This value decreased to around 47° at the end of 1000 cycles. As a result, it was determined that the GO electrode showed capacitive behavior.

The CV curves of the electrode Ni-doped GO at different scanning speeds in a 6 M KOH solution are given in Figure 8.

The reduction and oxidation peaks observed around -0.6 and -0.2 with the addition of Ni to the structure are not observed. The shape of the curves is quite similar to the rectangular shape observed in ideal capacitors [33-35].

Figure 9 is the first ten charge-discharge curves taken in a three-electrode cell within 6 M KOH of the Ni-doped GO electrode. While the addition of Ni to the structure does not create a difference in the potential value of charge-discharge, it has caused an increase in charge-discharge time.

The electrochemical impedance spectroscopy results are given in Figure 10. The slope of the curve is around 63°. As a result, adding Ni to the structure has improved the capacitive properties of GO electrodes by producing the modified Hummers method.

In Fig 11, the change of the specific capacitance of the GO and Ni-doped GO 360 electrodes with a charge-discharge cycle is given. The charge-discharge tests were performed at 1 Ag^{-1} for both electrodes. The specific capacitance of the GO electrode, which was 181 Fg-1 at the beginning, decreased to 166 Fg^{-1} after 1000 cycles of charge-discharge. The initial capacitance of the Ni-doped GO 360 electrode decreased from 246 Fg^{-1} to 187 Fg^{-1} after 1000 cycles. The addition of Ni to the structure and the application of heat treatment increased the surface area, as well as increased the specific capacitance accurately.

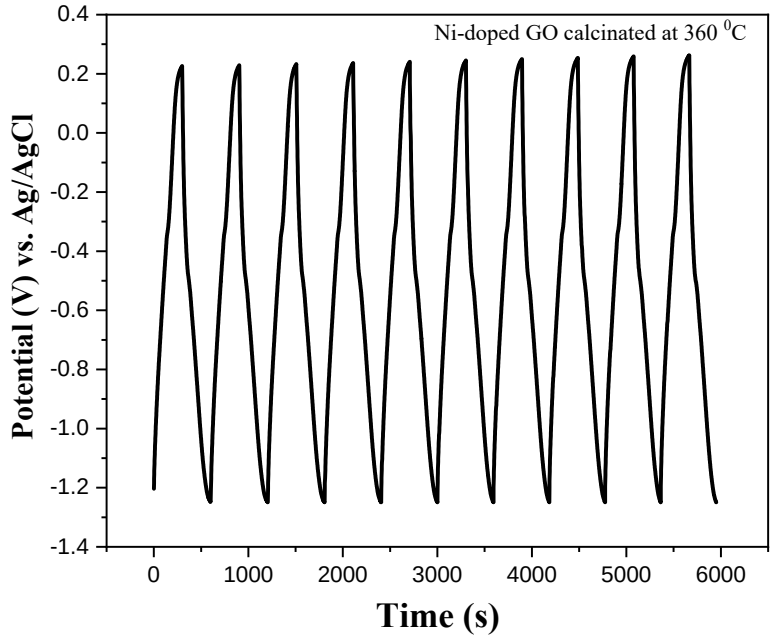

Figure 9. The first ten charge-discharge curves of the Ni-doped GO electrode.

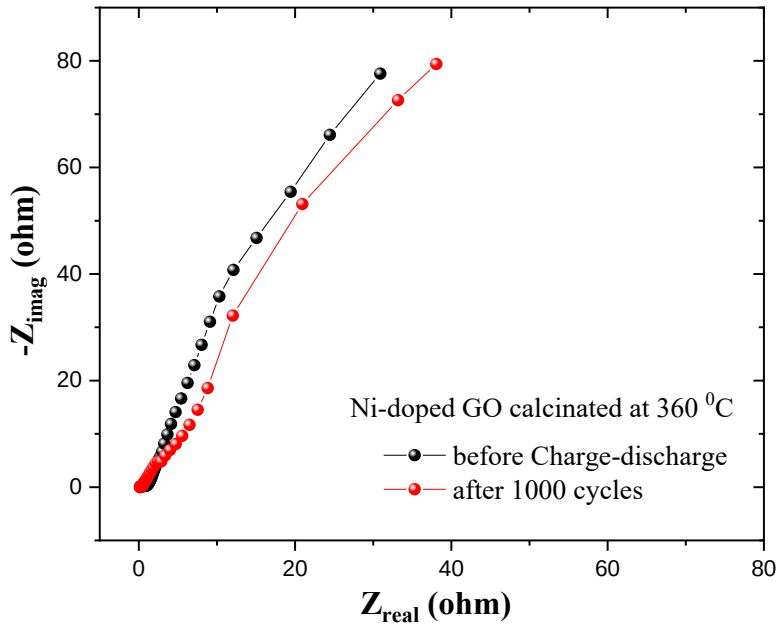

Figure 10. Electrochemical impedance spectroscopy curves at the open circuit potential of the Ni-doped GO 360 electrode.

4. Conclusion

In this study, nickel was added to the graphene oxide structure obtained by the modified Hummers method and heat treatment was applied at 360°C. It has been determined from XRD that the nickel contained in the structure is transformed into a NiO structure as a result of heat treatment. In addition, the surface area of the structure obtained by nickel doping and heat treatment has increased from 3 m^2 g^{-1} to 228 m^2 g^{-1}. While the specific capacitance of GO produced by Hummer was 166 F/g, it increased to 187 F/g as a result of the addition of Nickel to the structure. However, an increase in specific capacitance has also been observed as a result of nickel doping and heat treatment. After long-term charge-discharge tests, it was found that the Ni-doped GO 360 electrode retained 76% of its initial capacitance.

Conflict of Interest

The authors report no conflict of interest relevant to this article.

Research and Publication Ethics Statement

The authors declare that this study complies with research and publication ethics

References

[1] Moosa, A., and Abed, M. (2021). Graphene preparation and graphite exfoliation. *Turkish Journal of Chemistry*, 45(3), 493-519.

[2] Brisebois, P. P., and Siaj, M. (2020). Harvesting graphene oxide–years 1859 to 2019: a review of its structure, synthesis, properties and exfoliation. *Journal of Materials Chemistry C*, 8(5), 1517-1547.

[3] Paulchamy, B., Arthi, G., and Lignesh, B. D. (2015). A simple approach to stepwise synthesis of graphene oxide nanomaterial. *J Nanomed Nanotechnol*, 6(1), 1.

[4] Sun, L., and Fugetsu, B. (2013). Mass production of graphene oxide from expanded graphite. *Materials Letters*, 109, 207-210.

[5] Lalire, T., Otazaghine, B., Taguet, A., and Longuet, C. (2022). Correlation between multiple chemical modification strategies on graphene or graphite and physical/electrical properties. *FlatChem*, 33, 100376.

[6] Nimbalkar, A. S., Tiwari, S. K., Ha, S. K., and Hong, C. K. (2020). An efficient water saving step during the production of graphene oxide via chemical exfoliation of graphite. *Materials Today: Proceedings*, 21, 1749-1754.

[7] Song, Y., Zou, W., Lu, Q., Lin, L., and Liu, Z. (2021). Graphene transfer: Paving the road for applications of chemical vapor deposition graphene. *Small*, 17(48), 2007600.

[8] Zhang, J., Wang, F., Shenoy, V. B., Tang, M., and Lou, J. (2020). Towards controlled synthesis of 2D crystals by chemical vapor deposition (CVD). *Materials Today*, 40, 132-139.

[9] Li, C. B., Li, Y. J., Zhao, Q., Luo, Y., Yang, G. Y., Hu, Y., and Jiang, J. J. (2020). Electromagnetic interference shielding of graphene aerogel with layered microstructure fabricated via mechanical compression. *ACS Applied Materials and Interfaces*, 12(27), 30686-30694.

[10] Pastore Carbone, M. G., Manikas, A. C., Souli, I., Pavlou, C., and Galiotis, C. (2019). Mosaic pattern formation in exfoliated graphene by mechanical deformation. *Nature Communications*, 10(1), 1572.

[11] Salverda, M., Thiruppathi, A. R., Pakravan, F., Wood, P. C., and Chen, A. (2022). Electrochemical exfoliation of graphite to graphene-based nanomaterials. *Molecules*, 27(24), 8643.

[12] Pingale, A. D., Owhal, A., Katarkar, A. S., Belgamwar, S. U., and Rathore, J. S. (2021). Facile synthesis of graphene by ultrasonic-assisted electrochemical exfoliation of graphite. *Materials Today: Proceedings*, 44, 467-472.

[13] Laçin, Ö., and Dönmez, B. (2021). Modifiye Hummers Yöntemi ile Elde Edilen Grafen Oksit Sentezleri İçin: Kısım3, Fourier Dönüşümlü Kızılötesi Spektroskopisi Analizi. *Avrupa Bilim ve Teknoloji Dergisi*, (28), 985-989.

[14] Dreyer, D. R., Park, S., Bielawski, C. W., and Ruoff, R. S. (2010). The chemistry of graphene oxide. *Chemical Society Reviews*, 39(1), 228-240.

[15] Lavin-Lopez, M. D. P., Romero, A., Garrido, J., SanchezSilva, L., and Valverde, J. L. (2016). Influence of different improved hummers method modifications on the characteristics of graphite oxide in order to make a more easily scalable method. *Industrial and Engineering Chemistry Research*, 55(50), 12836-12847.

[16] Koçak, B., and Çelikkan, H. (2021). A novel and highly sensitive reduced graphene oxide modified electrochemical sensor for the determination of chlorpyrifos in real sample. *International Journal of Pure and Applied Sciences*, 7(1), 1-12.

[17] Marcano, D. C., Kosynkin, D. V., Berlin, J. M., Sinitskii, A., Sun, Z., Slesarev, A., Alemany, L.B., Lu, W., and Tour, J. M. (2010). Improved synthesis of graphene oxide. *ACS Nano*, 4(8), 4806-4814.

[18] Niu, Y., Zhang, Q., Li, Y., Fang, Q., and Zhang, X. (2017). Reduction, dispersity and electrical properties of graphene oxide sheets under low-temperature thermal treatments. *Journal of Materials Science: Materials in Electronics*, 28, 729-733.

[19] Wojtoniszak, M., Chen, X., Kalenczuk, R. J., Wajda, A., Łapczuk, J., Kurzewski, M., and Borowiak-Palen, E. (2012). Synthesis, dispersion, and cytocompatibility of graphene oxide and reduced graphene oxide. *Colloids and Surfaces B: Biointerfaces*, 89, 79-85.

[20] Aliyev, E., Filiz, V., Khan, M. M., Lee, Y. J., Abetz, C., and Abetz, V. (2019). Structural characterization of graphene oxide: Surface functional groups and fractionated oxidative debris. *Nanomaterials*, 9(8), 1180.

[21] Surekha, G., Krishnaiah, K. V., Ravi, N., and Suvarna, R. P. (2020, March). FTIR, Raman and XRD analysis of graphene oxide films prepared by modified Hummers method. *In Journal of Physics: Conference Series* (Vol. 1495, No. 1, p. 012012). IOP Publishing.

[22] Adel, M., Ahmed, M. A., Elabiad, M. A., and Mohamed, A. A. (2022). Removal of heavy metals and dyes from wastewater using graphene oxide-based nanomaterials: A critical review. *Environmental Nanotechnology, Monitoring and Management*, 18, 100719.

[23] Chao, D., and Fan, H. J. (2019). Intercalation pseudocapacitive behavior powers aqueous batteries. *Chem*, 5(6), 1359-1361.

[24] Munteshari, O., Lau, J., Likitchatchawankun, A., Mei, B. A., Choi, C. S., Butts, D., Dunn, B.S., and Pilon, L. (2019). Thermal signature of ion intercalation and surface redox reactions mechanisms in model pseudocapacitive electrodes. *Electrochimica Acta*, 307, 512-524.

[25] Jiang, Y., and Liu, J. (2019). Definitions of pseudocapacitive materials: a brief review. *Energy and Environmental Materials*, 2(1), 30-37.

[26] Surendran, V., Arya, R. S., Vineesh, T. V., Babu, B., and Shaijumon, M. M. (2021). Engineered carbon electrodes for high performance capacitive and hybrid energy storage. *Journal of Energy Storage*, 35, 102340.

[27] Joshi, B., Samuel, E., Kim, Y. I., Yarin, A. L., Swihart, M. T., and Yoon, S. S. (2021). Electrostatically sprayed nanostructured electrodes for energy conversion and storage devices. *Advanced Functional Materials*, 31(14), 2008181.

[28] Sitaaraman, S. R., Santhosh, R., Kollu, P., Jeong, S. K., Sellappan, R., Raghavan, V., Jacob, C., and Grace, A. N. (2020). Role of graphene in NiSe2/graphene composites-Synthesis and testing for electrochemical supercapacitors. *Diamond and Related Materials*, 108, 107983.

[29] Ahmed, A., Rafat, M., and Ahmed, S. (2020). Activated carbon derived from custard apple shell for efficient supercapacitor. *Advances in Natural Sciences: Nanoscience and Nanotechnology*, 11(3), 035013.

[30] Yavarian, M., Melnik, R., and Mišković, Z. L. (2023). Modeling of charging dynamics in electrochemical systems with a graphene electrode. *Journal of Electroanalytical Chemistry*, 946, 117711.

[31] Tanwar, S., Singh, N., and Sharma, A. L. (2022). Structural and electrochemical performance of carbon coated molybdenum selenide nanocomposite for supercapacitor applications. *Journal of Energy Storage*, 45, 103797.

[32] Laschuk, N. O., Easton, E. B., and Zenkina, O. V. (2021). Reducing the resistance for the use of electrochemical impedance spectroscopy analysis in materials chemistry. *RSC Advances*, 11(45), 27925-27936.

[33] Yuan, Y., Yuan, W., Wu, Y., Wu, X., Zhang, X., Jiang, S., Zhao, B., Chen, Y., Yang, C., Ding, L., Tang, Z., Xie, Y., and Tang, Y. (2023). High-Performance all-printed flexible micro-supercapacitors with hierarchical encapsulation. *Energy and Environmental Materials*, e12657.

[34] Liang, T., Mao, Z., Li, L., Wang, R., He, B., Gong, Y., Jin, J., Yan, C., and Wang, H. (2022). A mechanically flexible necklace-like architecture for achieving fast charging and high capacity in advanced lithium-ion capacitors. *Small*, 18(27), 2201792.

[35] Gharbi, O., Tran, M. T., Tribollet, B., Turmine, M., and Vivier, V. (2020). Revisiting cyclic voltammetry and electrochemical impedance spectroscopy analysis for capacitance measurements. *Electrochimica Acta*, 343, 136109.